



Research paper

Breaking dendrites of lithium metal electrode by resonance: A theoretical calculation of lattice dynamics

Han Zhou^a, Hailong Wang^b, Xiaohui Ning^{a,*}

^a Center for Advancing Materials Performance from the Nanoscale (CAMP-Nano), State Key Laboratory Behavior of Materials, School of Materials Science and Engineering, Xi'an Jiaotong University, Xi'an, Shanxi 710049, PR China

^b School of Physics Electrical Information Engineering, Ningxia University, Yinchuan, Ningxia 750021, PR China

ARTICLE INFO

Keywords:

Lattice dynamics
MAEAM
Phonon spectrum
Resonance
Lithium dendrites

ABSTRACT

The phonon spectrum and resonance are studied by lattice dynamics and the modified analytic embedded-atom method. The phonon spectrum of lithium is calculated along three principal directions. The calculated and experimental values are in good agreement. Moreover, the phonon dispersion of acoustic wave is added to the phonon spectrum of lithium metal and the transverse and longitudinal waves of resonance frequencies are calculated. It is proposed that acoustic wave could resonance with metal lithium electrodes and break the detrimental lithium dendrites. Otherwise the resonance could be controlled in each direction by adjusting the frequency, thus changing other properties of lithium.

1. Introduction

Metallic lithium plays a pivot role in many industrial applications such as aerospace nuclear plant and battery materials. Particularly, lithium metal electrode is an essential part of battery industry and is the most promising anode material because of its most negative normal electrode potential (-3.040 V vs the standard hydrogen electrode) and the ultra-high capacity (3860 mAh/g), so that lithium metal is regarded as a "Holy Grail" electrode and has received extensive attentions [1-3]. Batteries adopting metal lithium as negative poles are likely to become the next generation of high energy storage device [2]. However, the growth of uncontrolled lithium dendrites [1] and limited coulombic efficiency [1] result in poor cycling efficiency, severe safety concerns, and poor lifespan, which severely prevents the practical applications of lithium metal based batteries. To address this issue, various methods from the aspect of chemistry of materials have been proposed [4], for example, highly concentrated electrolytes [5], 'Solvent-in-Salt' electrolytes [6], carbon-coated lithium metal anode [7,8], selection of electrolyte additives (film forming additives includes FEC [9,10], VC [11,12], deposition additives includes Cesium ion [13]), constructing solid electrolyte interphase (SEI) [14,15], chemical pretreatment (gas-phase treatment [16,17], liquid-phase treatment [15,18]), electrochemical retreatment [19-21], physical pretreatment [22], negative surface protection (LiF [23], LiPO₄ [24]), and negative skeleton

structure design (Lithiophilic skeleton [25-27], conductive skeleton [28,29]).

Dendrites growth is generally unstable and fragile in the experience of metallurgy science, which can be easily disrupted or broken by convections and vibrations. The resonance vibration could be devastating for the nucleation and growth of lithium dendrite from the dandling bonds of lithium metal surface. The resonance vibration can be exerted by external devices during Li ions' reduction on the lithium metal anode (charging process) to inhibit the formation of detrimental lithium dendrites. Calculating accurate resonance data for anisotropic lithium metal crystalline and optimizing the external resonance are therefore the work of top priority.

The phonon spectrum is the basis for calculation of the resonance frequency of metals. Many methods have been developed to measure the phonon spectrum which include Far-Infrared and Infrared Spectroscopy (FIR and IR) [30], Raman Spectroscopy (R) [30], Brillouin Spectroscopy (B) [30], Diffuse X-Ray Scattering [30] and Inelastic Neutron Scattering (INS) [30]. Theoretical calculation of the Lithium metal's resonance frequencies is still deficient and it could remedy the lack of experiment measuring, where the calculation of phonon spectrum of lithium metal is imperative.

There are many methods for calculating phonon spectrums, for instance, pair potentials [31-33], the general tensor force model [34], the embedded atom method (EAM) [35], analytic EAM (AEAM) [36,37],

* Corresponding author.

E-mail address: xiaohuining@mail.xjtu.edu.cn (X. Ning).

<https://doi.org/10.1016/j.cplett.2021.138921>

Received 7 May 2021; Received in revised form 25 July 2021; Accepted 26 July 2021

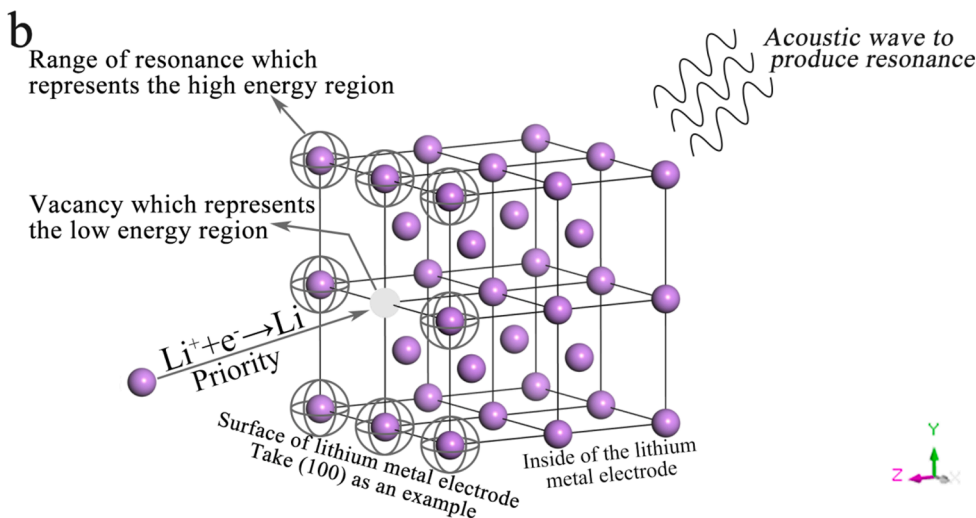
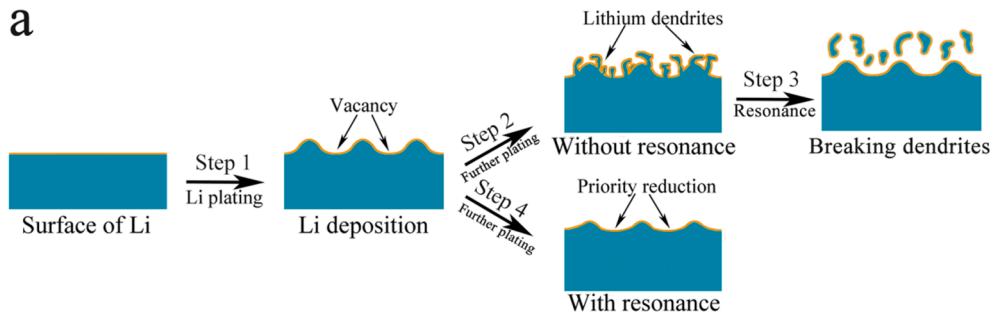
Available online 29 July 2021

0009-2614/© 2021 Elsevier B.V. All rights reserved.

ab initio [38-41], and pseudopotential theory [42]. Based on EAM, MAEAM developed by Zhang et al. [43] is more accurate because it proposed the expression of energy correction term [44] which is used to describe the energy deviation caused by the deviation of electron density from the spherically symmetric distribution and it provides an analytical expression of interatomic potential functions [43] which can describe various metal structures. In this paper, we have used MAEAM method to calculate the phonon spectrums of lithium metal in [1 0 0], [1 1 0] and [1 1 1] directions. The calculated results and experimental values measured by H.G. Smith et al. [44] are in good agreement.

Calculating resonance by phonon spectrums has already been used in ionic crystals. By calculating the phonon spectrums of ionic crystals, the conditions for resonance with electromagnetic waves can be obtained [45]. Therefore, long optical waves of ionic crystals can resonate with far-infrared rays, which has been widely used [45]. Presented in this paper, similarly, we calculate the phonon spectrum of lithium metal by MAEAM method and the conditions of resonance between lithium metal and acoustic wave in [1 0 0], [1 1 0] and [1 1 1] directions. Specially, we discuss the resonance of acoustic wave propagated in air with lithium atom at room temperature and calculate the conditions of resonance between lithium metal and acoustic wave in [1 1 1] directions.

Through resonance, the surface resonance of lithium metal electrode is intensified during charging, so that lithium ions are preferentially reduced in the vacant position, and inhibit the growth of lithium dendrite ultimately. The vacancy could be produced by two reasons. One reason is the lithium deintercalation during discharging. Another reason is the non-uniform Li deposition [49] during charging which is shown in Fig. 1a. We consider the surface of lithium metal electrode in an ideal state and take (100) as an example, which is shown in Fig. 1b.



2. Methods

2.1. Maeam

According to MAEAM [43], which takes into account the next-nearest neighbor proposed by Zhang et al., the basic formula of the modified analytical embedded atomic method for lithium metal is obtained as follows [43]:

$$E_t = \sum_i F(\rho_i) + \frac{1}{2} \sum_i \sum_{j \neq i} \varphi(r_{ij}) + \sum_i M(P_i) \quad (1)$$

$$\rho_i = \sum_{j \neq i} f(r_{ij}) \quad (2)$$

$$P_i = \sum_{j \neq i} f^2(r_{ij}) \quad (3)$$

where E_t is the total energy of the system, ρ_i is the density of electrons produced by all other atoms at atom i , P_i is the contribution of non-spherical symmetry to electron density of atoms in real crystals.

$F(\rho_i)$ is the "embedding energy" function (energy required to embed an atom in the background electron density ρ_i at site i), $\varphi(r_{ij})$ is the interaction potential between atom i and atom j , $M(P_i)$ is the modified term which describes the energy change due to nonlinear superposition of atomic electronic density, $f(r_{ij})$ is the electron density of atom j at atom i , and r_{ij} is the separation distance of atom i from atom j . $F(\rho_i)$, $\varphi(r_{ij})$, $M(P_i)$ and $f(r_{ij})$ are given by [43]:

$$F(\rho_i) = -F_0 \left[1 - \ln \left(\frac{\rho_i}{\rho_c} \right) \left(\frac{\rho_i}{\rho_c} \right)^n \right] \quad (4)$$

$$\varphi(r_{ij}) = l_0 + l_1 \left(\frac{r_{ij}}{r_{2e}} - 1 \right) + l_2 \left(\frac{r_{ij}}{r_{2e}} - 1 \right)^2 + l_3 \left(\frac{r_{ij}}{r_{2e}} - 1 \right)^3 \quad (5)$$

Fig. 1. a, The surface changing process of lithium metal electrode with/without resonance. Step 1: The non-uniform Li deposition [49]. Step 2: Formation of lithium dendrites [49]. Step 3: Resonance could break the lithium dendrites directly. Step 4: With resonance, Li uniformly deposited on the surface. b, The uniform Li deposition with resonance. Acoustic wave to produce resonance and the surface of lithium metal in (100) crystal plane where the lithium ions are preferentially reduced in the vacant position during charging.

$$M(P_i) = \alpha \left(\frac{P_i}{P_e} - 1 \right)^2 \exp \left[- \left(\frac{P_i}{P_e} - 1 \right)^2 \right] \quad (6)$$

$$f(r_{ij}) = f_e \left(\frac{r_{1e}}{r_{ij}} \right)^\beta \quad (7)$$

where the subscript “e” represents equilibrium state and r_{1e} , r_{2e} , r_{3e} are the first, the second and the third nearest neighbor distance at equilibrium. $\beta \approx 6$. We discussed the calculation of the phonon dispersion relationship of lithium metal by MAEAM considering the next-nearest neighbor. Therefore, $\varphi(r_{ij})$ is selected to $r < r_{2e}$.

F_0 , f_e , ρ_i , P_e are the calculated model parameters which are given by [43]:

$$F_0 = E_c - E_{1v} \quad (8)$$

$$f_e = [(E_c - E_{1v})/\Omega]^{3/5} \quad (9)$$

$$\rho_e = N_1 f_1 + N_2 f_2 \quad (10)$$

$$P_e = N_1 f_1^2 + N_2 f_2^2 \quad (11)$$

$$f_1 = f(r_{1e}) \quad (12)$$

$$f_2 = f(r_{2e}) \quad (13)$$

where E_c is the cohesion energy, E_{1v} is the mono-vacancy formation energy, Ω is the volume of primitive cell.

There are the following MAEAM model parameters for lithium metal [46-48], and calculated parameters shown in Table 1 and 2:

2.2. Lattice dynamics

It is known that the total potential energy of an atomic system is a function of the instantaneous potential vectors of all atoms:

$$E = E[\dots + r(l) + u(l) + \dots] \quad (14)$$

where $r(l)$ is the equilibrium potential vector of atom l , $u(l)$ is the instantaneous displacement of the equilibrium position of atom l . In the case of small displacement, the three-dimensional Taylor expansion of the potential energy at the equilibrium position is carried out and the atomic motion equation is obtained under the harmonic approximation:

$$m u_\alpha(l) = - \sum_{\beta k} \varphi_{\alpha\beta}(l, k) u_\beta(k) \quad (15)$$

Table 1
Calculated parameters for lithium metal.

Parameters	Li
Li	
The coordination numbers of the first shell N_1	8
The coordination numbers of the second shell N_2	6
The volume of primitive cell Ω , nm ³	0.0216
Model parameters F_0 , eV	1.2150
Model parameters l_0 , eV	-0.0593
Model parameters l_1 , 10 ⁻⁴ eV	7.7057
Model parameters k_0 , eV	
Model parameters l_2 , eV	1.8372
Model parameters l_3 , eV	-3.9453
Model parameters n	0.1130
Model parameters α	-0.0019

Table 2
MAEAM model parameters for lithium metal [46-48].

Parameters	Li	Ref.
Lattice constant a , nm	0.3509	[46]
Mono-vacancy formation energy E_{1v} , eV	0.4150	[47]
Cohesion energy E_c , eV	1.6300	[46]
Elastic constant C_{11} , eV/nm ³	92.500	[48]
Elastic constant C_{12} , eV/nm ³	78.125	[48]
Elastic constant C_{44} , eV/nm ³	67.500	[48]

where m is the atomic mass, $\alpha, \beta = x, y, z$ (components of cartesian coordinates), $\varphi_{\alpha\beta}(l, k)$ is the atomic force constants, representing the force acting on atom l in the direction while atom k moves a unit displacement in the direction β , which can be calculated by evaluating the second derivatives of the total energy of a system E_t with respect to the atoms coordinates:

$$\varphi_{\alpha\beta}(l, k) = \frac{\partial^2 E_t}{\partial u_\alpha(l) \partial u_\beta(k)} \quad (16)$$

Substitute (14) into (13):

$$m \omega^2 A_\alpha(l) = \sum_{k, \beta} A_\beta(k) \varphi_{\alpha\beta}(l, k) \exp\{-i\vec{q} \cdot [\vec{r}(k) - \vec{r}(l)]\} \quad (17)$$

The dynamic matrix is defined as:

$$D_{\alpha\beta}(l, k) = \sum_k \varphi_{\alpha\beta}(l, k) \exp\{-i\vec{q} \cdot [\vec{r}(k) - \vec{r}(l)]\} \quad (18)$$

Substitute (16) into (15):

$$\sum_\beta D_{\alpha\beta}(l, k) A_\beta(k) - m \omega^2 (\vec{q}) A_\alpha(l) = 0 \quad (19)$$

where (17) is the secular equation, $A_\alpha(l)$, $A_\beta(k)$ are the amplitude of atom l in direction α and the amplitude of atom k in direction β , q is the three-dimensional wave vector, $r(l)$, $r(k)$ are the displacement vectors of atom l and atom k . In harmonic approximation, the normal mode phonon frequencies ω corresponding to a wave vector q can be calculated by solving the secular equation.

In this paper, lithium metal with body-centered cubic structure considers the first and the second nearest neighbors. The first nearest neighbor force constants ($\alpha = |\varphi_{\alpha\beta}(l, 1)|$) and the second nearest neighbor force constants ($\beta = |\varphi_{\alpha\beta}(l, 9)|$) need to be calculated. Assuming that there is only two-body central force and the equilibrium position of atom l is the coordinate origin, so the central atom is forced by 8 neighboring and 6 next-neighboring atoms and the following formulas are obtained:

$$\left\{ \begin{aligned}
D_{xx}(l, k) &= \varphi_{xx} + \sum_{k=1}^{14} \varphi_{xx}(l, k) e^{-i\vec{q} \cdot \vec{r}(k)} D_{yy}(l, k) \\
&= \varphi_{yy} + \sum_{k=1}^{14} \varphi_{yy}(l, k) e^{-i\vec{q} \cdot \vec{r}(k)} D_{zz}(l, k) \\
&= \varphi_{zz} + \sum_{k=1}^{14} \varphi_{zz}(l, k) e^{-i\vec{q} \cdot \vec{r}(k)} D_{xy}(l, k) \\
&= \varphi_{xy} + \sum_{k=1}^{14} \varphi_{xy}(l, k) e^{-i\vec{q} \cdot \vec{r}(k)} D_{xz}(l, k) \\
&= \varphi_{xz} + \sum_{k=1}^{14} \varphi_{xz}(l, k) e^{-i\vec{q} \cdot \vec{r}(k)} D_{yz}(l, k) = \varphi_{yz} + \sum_{k=1}^{14} \varphi_{yz}(l, k) e^{-i\vec{q} \cdot \vec{r}(k)} \quad (20)
\end{aligned} \right.$$

where φ_{xx} , φ_{yy} , φ_{zz} , φ_{xy} , φ_{xz} , φ_{yz} are the central atom l forces itself on \times , y , z , x , y , z , x , y , z , z , y , z , z directions. Assuming that the equilibrium positions of 8 neighboring and 6 next-neighboring atoms are:

$$\begin{aligned}
&\pm \left(\frac{a}{2}, \frac{a}{2}, \frac{a}{2} \right), \pm \left(\frac{a}{2}, \frac{a}{2}, -\frac{a}{2} \right), \pm \left(\frac{a}{2}, -\frac{a}{2}, \frac{a}{2} \right), \pm \left(-\frac{a}{2}, \frac{a}{2}, \frac{a}{2} \right), \\
&\pm (a, 0, 0), \pm (0, a, 0), \pm (0, 0, a) \quad (21)
\end{aligned}$$

By calculating the expressions of each dynamic matrix and putting them into (17), we get $\omega(q)$ which is dispersion relations:

Wave vector q in [100] direction:

$$\left\{ \begin{aligned}
\omega_1^2 &= \frac{4}{m} \left[\beta \sin^2 \frac{a}{2} q + 4 \alpha \sin^2 \frac{a}{4} q \right] \\
\omega_{2,3}^2 &= \frac{16}{m} \alpha \sin^2 \frac{a}{4} q
\end{aligned} \right. \quad (22)$$

Wave vector q in [110] direction:

$$\left\{ \begin{aligned}
\omega_1^2 &= \frac{8}{m} \alpha \sin^2 \frac{\sqrt{2}}{4} a q \\
\omega_2^2 &= \frac{4}{m} (4\alpha + \beta) \sin^2 \frac{\sqrt{2}}{4} a q \\
\omega_3^2 &= \frac{4}{m} \beta \sin^2 \frac{\sqrt{2}}{4} a q
\end{aligned} \right. \quad (23)$$

Wave vector q in [111] direction:

$$\left\{ \begin{aligned}
\omega_{1,2}^2 &= \frac{4}{m} \left(\beta \sin^2 \frac{\sqrt{3}}{6} a q + 4 \alpha \sin^2 \frac{\sqrt{3}}{12} a q \right) \\
\omega_3^2 &= \frac{4}{m} \left(\beta \sin^2 \frac{\sqrt{3}}{6} a q + 3 \alpha \sin^2 \frac{\sqrt{3}}{4} a q + \alpha \sin^2 \frac{\sqrt{3}}{12} a q \right)
\end{aligned} \right. \quad (24)$$

Substitute E_t into (14), we get:

$$\Phi(i, j) = \varphi''(r_{ij}) + 2F'(\rho_i) f''(r_{ij}) + F''(\rho_i) f'(r_{ij})^2 + 4M'(P_i) [f(r_{ij}) f'(r_{ij}) + f'(r_{ij})^2] + 4M''(P_i) f(r_{ij})^2 f'(r_{ij})^2 \quad (25)$$

where r_{ij} is the separation distance of atom i from atom j :

$$\left\{ \begin{aligned}
r_{ij} &= r_{1e} + u(j) - u(i) \\
r_{ij} &= r_{2e} + u(j) - u(i)
\end{aligned} \right. \quad (26)$$

Then the frequencies ω can be obtained by solving (23).

3. Results and discussion

3.1. Phonon dispersion of lithium

The calculated phonon dispersion curves, the available experimental values [44] and the calculated results of Guellil and Adams [36] for lithium metal in three directions of [100], [110], [111] are shown in Fig. 2a-2c, respectively. For bcc metal, the phonon spectrums only have acoustic branches [45] which include transverse branch and longitudinal branch. In Fig. 2a, the black lines represent the longitudinal branches which vibrate along [100] direction, and the red lines represent the transverse branches which vibrate perpendicular to [100] direction. In Fig. 2b, the black lines represent the longitudinal branches which vibrate along [110] direction. The two red lines represent transverse branches. One vibrates along [001] direction and spreads along [110] direction, and the other vibrates along [1-10] direction and spreads along [110] direction. In Fig. 2c, the black lines represent the longitudinal branches which vibrate along [111] direction, and the red lines represent the transverse branches which vibrate perpendicular to [111] direction.

The calculated phonon dispersion curves reproduced very well the available experimental results. In [100] and [110] directions, the calculated and experimental values are in better agreement than the results of Guellil and Adams [36]. In [111] direction, the curves have a shape which is very similar to that found experimentally, though the actual degree of fit varies somewhat. Partly reasons are the present calculations are within harmonic approximations, and the experimental values are obtained at a temperature where the anharmonic effects are not negligible instead. In short, the theoretical and experimental data are in good agreement by using MAEAM methods.

3.2. Resonance

For resonance with acoustic waves, we combine the acoustic dispersion with phonon dispersion of Li and get the slope of a certain range which are the conditions of resonance. The dispersion relation of acoustic wave can be calculated by:

$$\omega = v \cdot q \quad (27)$$

where v is the velocity of acoustic wave and also the slope of the dispersion relation. The acoustic wave velocity is changed in different mediums. Therefore, the different slopes represent the acoustic wave velocities in different mediums and we calculate the certain velocities which can resonance with metal lithium. The results are shown in Fig. 3a-3g.

Where k_{max} and k_{min} represent the maximum and minimum slope of

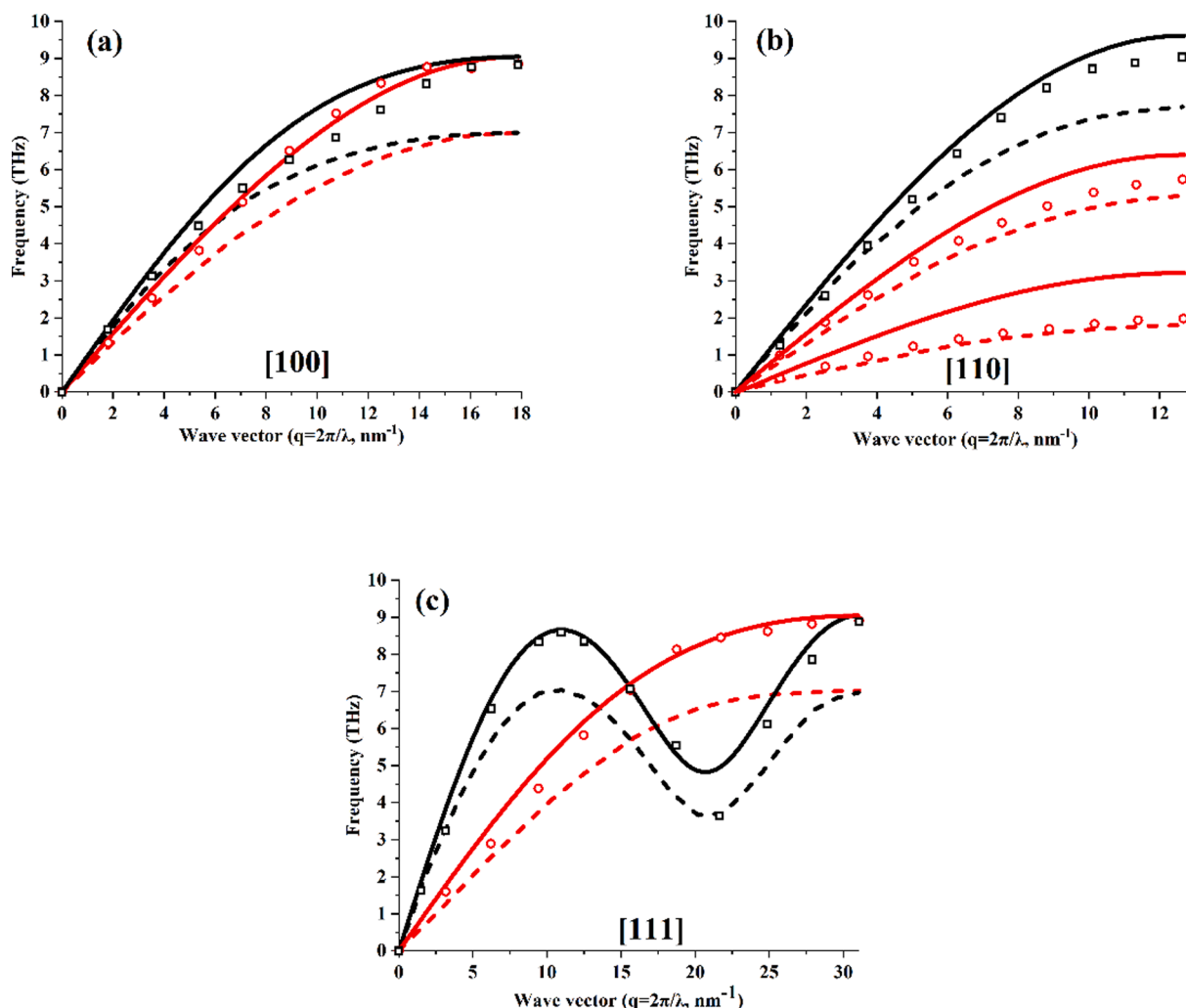


Fig. 2. Phonon dispersion of Li in (a)[100], (b)[110] and (c)[111] directions. The solid lines represent the calculated results, the various symbols represent experimental data [44] and the dashed lines represent the calculated results of Guellil and Adams [36].

calculated curve. According to (25), the slope k is the velocity. Therefore, we can calculate the range of velocity which is actually the condition of resonance. We summarize the above results in Table 3:

The acoustic wave velocity is changed in different mediums, and the certain velocity can be selected from Table 3.

In addition, we can calculate the frequency of the acoustic wave through the velocity of acoustic wave in the certain medium. Specially, the propagation velocity of acoustic wave in air is approximately 340 m/s at room temperature. According to Table 3, resonance occurs in [111] and [110] direction. Taking the [111] direction as an example, the results are shown in Fig. 4.

The black and red solid point are the conditions of resonance which are the certain frequencies 5.91×10^{12} Hz in transverse wave and 8.91×10^{12} Hz in longitudinal wave.

It means when acoustic wave contacts lithium in the air, if the frequency of the acoustic wave is 5.91×10^{12} Hz, the resonance condition is satisfied in [111] direction. The metal lithium will have a strong resonance with the acoustic wave, and the metal lithium atom will vibrate violently along the [111] direction. Similarly, if the frequency of the acoustic wave is 8.91×10^{12} Hz, the resonance condition is also satisfied. The metal lithium atoms will vibrate violently perpendicular to [111] direction. Therefore, there are two factors that affect lithium resonance with acoustic wave, frequency and velocity of the acoustic wave.

4. Conclusion

Combining the second nearest-neighbor modified analytic embedded-atom method (MAEAM) with lattice dynamics, we have calculated the expression of atomic force constants, and the phonon dispersion of lithium metal along directions [100], [110] and [111]. The calculated and experimental values are in good agreement. Through adding the phonon dispersion of acoustic wave to the phonon dispersion of lithium metal, we have calculated the conditions of resonance in these directions. Specially, we have calculated the conditions of resonance in the air. The results show that frequency and velocity of the acoustic wave are two factors affect the resonance. When these conditions are met, we mentioned that acoustic wave could be used to produce resonance with metal lithium electrodes to suppress the formation of lithium dendrites. We propose resonance will suppress the formation of lithium dendrites during during the charge process of Li batteries, meanwhile, if the lithium dendrite has already been formed, we can also break it by resonance. Otherwise the resonance could be controlled in each direction by adjusting the frequency and velocity, thus changing other properties of lithium. These methods can also help to study other metal electrodes.

CRediT authorship contribution statement

Han Zhou: Writing - original draft, Investigation, Methodology,

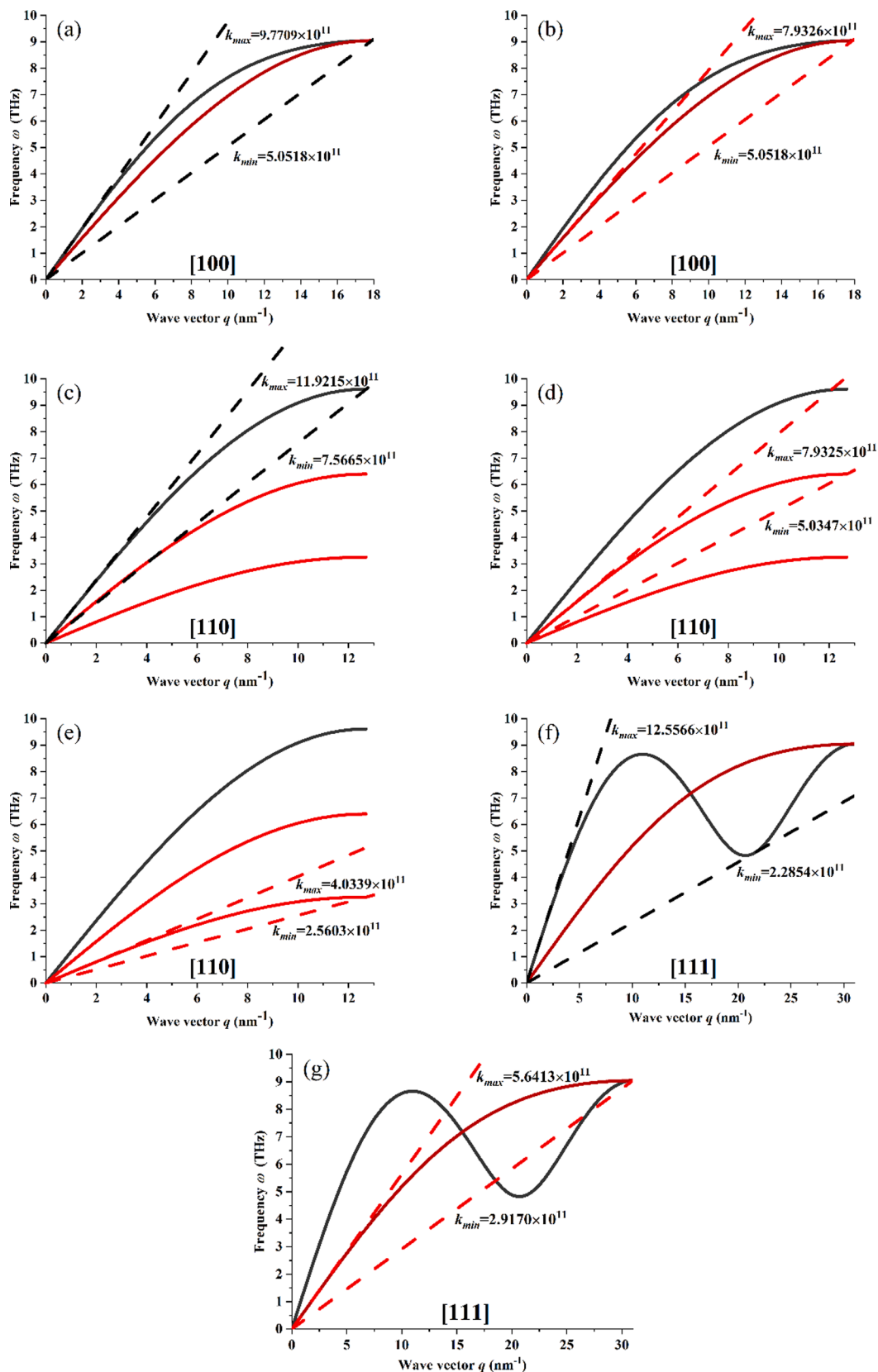


Fig. 3. Conditions of resonance in [100], [110] and [111] direction. The solid lines represent the calculated value and the dotted lines represent the resonance conditions. The black and red solid lines represent the longitudinal and transverse branch. (For interpretation of the references to colour in this figure legend, the reader is referred to the web version of this article.)

Table 3

The conditions of resonance with acoustic waves.

Direction	Condition	
[100]	Longitudinal branch (vibrate along [100] direction)	$505.18 \leq v \leq 977.09$
	Transverse branch (vibrate perpendicular to [100] direction)	$505.18 \leq v \leq 793.26$
	Longitudinal branch (vibrate along [110] direction)	$756.65 \leq v \leq 1192.15$
[110]	Longitudinal branch (vibrate along [110] direction)	$503.47 \leq v \leq 793.25$
	Transverse branch (vibrate along [001] direction)	$256.03 \leq v \leq 403.39$
	Transverse branch (vibrate along [1-10] direction)	$228.54 \leq v \leq 1255.66$
[111]	Longitudinal branch (vibrate along [111] direction)	$291.70 \leq v \leq 564.13$
	Transverse branch (vibrate perpendicular to [111] direction)	

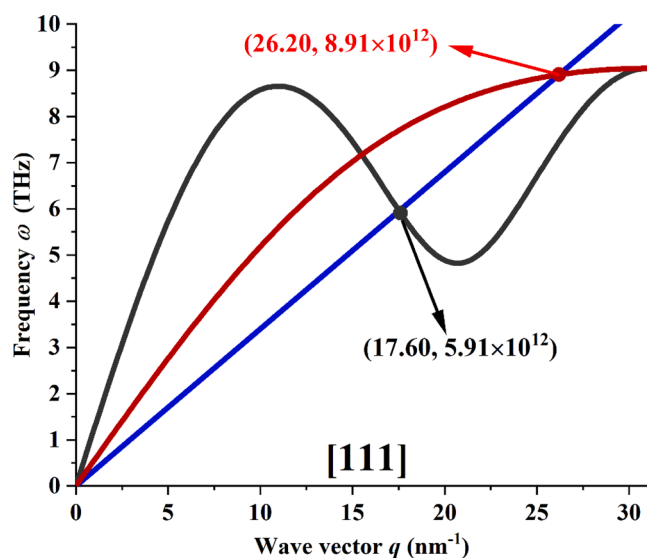
The velocity v is in m/s.

Fig. 4. Conditions of resonance with acoustic wave in [111] direction, the black, red and blue solid lines represent the longitudinal, transverse and acoustic waves, respectively. The black and red solid point are the intersections of curves which represent the conditions of resonance in longitudinal and transverse branches. (For interpretation of the references to colour in this figure legend, the reader is referred to the web version of this article.)

Conceptualization. **Hailong Wang**: Formal analysis, Data curation. **Xiaohui Ning**: Writing - review & editing, Supervision.

Declaration of Competing Interest

The authors declare that they have no known competing financial interests or personal relationships that could have appeared to influence the work reported in this paper.

Acknowledgements

The authors would like to acknowledge the financial support from National Natural Science Foundation of China (51874228, U1766216) and Natural Science Foundation of Shaanxi Province, China (2020JM-068).

References

- [1] W. Xu, J. Wang, F. Ding, X. Chen, E. Nasybulin, Y. Zhang, J. Zhang, *Energy Environ. Sci.* 7 (2014) 513.
- [2] Y. Sun, N. Liu, Y. Cui, *Nat. Energy.* 1 (2016) 16071.
- [3] X. Cheng, Q.J. Zhang, *Mater. Chem. A* 3 (2015) 7207.
- [4] X. Cheng, Q. Zhang, *Prog. Chem.* 30 (2018) 51.
- [5] Qian, J.; Henderson, W.; Xu, W. Bhattacharya, P.; Engelhard, M.; Borodin, O.; Zhang, J. *Nat. Commun.* 2015, 6, 6362.
- [6] L. Suo, Y. Hu, H. Li, M. Armand, L. Chen, *Nat. Commun.* 4 (2013) 1481.
- [7] G. Zheng, S. Lee, Z. Liang, H. Lee, K. Yan, H. Yao, H. Wang, W. Li, S. Chu, Y. Cui, *Nat. Nanotechnol.* 9 (2014) 618.
- [8] K. Yan, Z. Lu, H. Lee, F. Xiong, P. Hsu, Y. Li, J. Zhao, S. Chu, Y. Cui, *Nat. Energy.* 1 (2016) 16010.
- [9] H. Kuwata, H. Sonoki, M. Matsui, Y. Matsuda, N. Imanishi, *Electrochemistry* 84 (2016) 854.
- [10] J. Heine, P. Hilbig, X. Qi, P. Niehoff, M. Winter, P. Bieker, *J. Electrochem. Soc.* 162 (2015) A1094.
- [11] J. Guo, Z. Wen, M. Wu, J. Jin, Y. Liu, *Electrochem. Commun.* 51 (2015) 59.
- [12] H. Sano, H. Sakaebe, H. Matsumoto, *J. Power Sources* 196 (2011) 6663.
- [13] F. Ding, W. Xu, G. Graff, J. Zhang, M. Sushko, X. Chen, Y. Shao, M. Engelhard, Z. Nie, J. Xiao, X. Liu, P. Sushko, J. Liu, J. Zhang, *J. Am. Chem. Soc.* 135 (2013) 4450.
- [14] X. Cheng, R. Zhang, C. Zhao, F. Wei, J. Zhang, Q. Zhang, *Adv. Sci.* 3 (2016) 1500213.
- [15] N. Li, Y. Yin, C. Yang, Y. Guo, *Adv. Mater.* 2016 (1853) 28.
- [16] S. Koch, B. Morgan, S. Passerini, G. Teobaldi, *J. Power Sources* 296 (2015) 150.
- [17] D. Lin, Y. Liu, W. Chen, G. Zhou, K. Liu, B. Dunn, Y. Cui, *Nano Lett.* 17 (2017) 3731.
- [18] Y. Liu, D. Lin, P. Yuen, K. Liu, J. Xie, R. Dauskardt, Y. Cui, *Adv. Mater.* 29 (2017) 1605531.
- [19] Q. Liu, J. Xu, S. Yuan, Z. Chang, D. Xu, Y. Yin, L. Li, H. Zhong, Y. Jiang, J. Yan, X. Zhang, *Adv. Mater.* 27 (2015) 5241.
- [20] L. Ma, M. Kim, L. Archer, *Chem. Mater.* 29 (2017) 4181.
- [21] H. Wang, M. Matsui, H. Kuwata, H. Sonoki, Y. Matsuda, X. Shang, Y. Takeda, O. Yamamoto, N. Imanishi, *Nat. Commun.* 8 (2017) 15106.
- [22] Z. Peng, S. Wang, J. Zhou, Y. Jin, Y. Liu, Y. Qin, C. Shen, W. Han, D.J. Wang, *Mater. Chem. A* 4 (2016) 2427.
- [23] L. Fan, H. Zhuang, L. Gao, Y. Lu, L.J. Archer, *Mater. Chem. A* 5 (2017) 3483.
- [24] L. Wang, Q. Wang, W. Jia, S. Chen, P. Gao, J. Li, *J. Power Sources* 342 (2017) 175.
- [25] C. Jin, O. Sheng, J. Luo, H. Yuan, C. Fang, W. Zhang, H. Huang, Y. Gan, Y. Xia, C. Liang, J. Zhang, X. Tao, *Nano Energy* 37 (2017) 177.
- [26] X. Cheng, T. Hou, R. Zhang, H. Peng, C. Zhao, J. Huang, Q. Zhang, *Adv. Mater.* 28 (2016) 2888.
- [27] D. Lin, Y. Liu, Z. Liang, H. Lee, J. Sun, H. Wang, K. Yan, J. Xie, Y. Cui, *Nat. Nanotechnol.* 11 (2016) 626.
- [28] X. Cheng, H. Peng, J. Huang, R. Zhang, C. Zhao, Q. Zhang, *ACS Nano* 9 (2015) 6373.
- [29] C. Yang, Y. Yin, S. Zhang, N. Li, Y. Guo, *Nat. Commun.* 6 (2015) 8058.
- [30] P. Phonons Bruesch, *Theory and experiments II. Volume 2. Phonons, theory and experiments.* pp. 8 (1982) 173.
- [31] N. Singh, N. Banger, S. Singh, *Phys. Rev. B.* 39 (1989) 3097.
- [32] N. Singh, B. Yadav, *Phys. B.* 192 (1993) 205.
- [33] V. Vaks, E. Zarochevsev, S. Kravchuk, V. Safronov, A. Trefilov, *Phys. Status Solidi B.* 85 (1978) 63.
- [34] V. Ramamurthy, M. Satishkumar, *Phys. Rev. B.* 32 (1985) 5471.
- [35] S. Chantasiriwan, F. Milstein, *Phys. Rev. B* 58 (1998) 5996.
- [36] A. Guellil, J. Adams, *J. Mater. Res.* 7 (1992) 639.
- [37] W. Hu, M. Fukumoto, *Mater. Sci. Eng.* 10 (2002) 707.
- [38] V. Schott, M. Fähnle, P. Madden, *J. Phys.: Condens. Matter.* 12 (2000) 1171.
- [39] N. Christensen, D. Boers, J. van Velsen, D. Novikov, *J. Phys.: Condens. Matter.* 12 (2000) 3293.
- [40] W. Frank, C. Elsässer, M. Fähnle, *Phys. Rev. Lett.* 74 (1995) 1791.
- [41] Y. Xie, J. Tse, T. Cui, A. Oganov, Z. He, Y. Ma, G. Zou, *Phys. Rev. B.* 75 (2007), 064102.
- [42] J. Baria, *Physica B* 371 (2006) 280.
- [43] B. Zhang, Y. Ouyang, S. Liao, Z. Jin, *Physica B.* 262 (1999) 218.
- [44] H. Smith, G. Dolling, R. Nicklow, P. Vijayaraghavan, M. Wilkinson, *Symposium on neutron inelastic scattering, IAEA, Vienna, 1968.*
- [45] K. Huang, R. Han, *Solid Physics, Higher Education Press, Beijing, 1988.*
- [46] Y. Xie, J. Zhang, *Can. J. Phys.* 86 (2008) 801.
- [47] F.R. de Boer, *Cohesion in Metals: Transition Metal Alloys, North-Holland, Amsterdam, 1988.*
- [48] G. Simmons, H. Wang, *Single crystal elastic constants and calculated aggregate properties: a handbook, MIT, Cambridge, Mass. (1971).*
- [49] D. Lin, Y. Liu, C. Yi, *Nature Nanotech* 12 (2017) 194.